UDC 622.268.6 DOI: https://doi.org/10.15407/geotm2025.174.161

FINITE ELEMENT ANALYSIS OF DEFORMATION, GROUNDWATER FLOW, AND POLYMER INJECTION WITH ROCKBOLTS

Krukovska V.

M.S. Poliakov Institute of Geotechnical Mechanics of the National Academy of Sciences of Ukraine

Abstract. This study introduces a novel finite element model for simulating the coupled processes of rock deformation, groundwater inflow, and polymer injection during installation of injection rockbolts in weak water-bearing strata. The model integrates mechanical response of the rock mass, hydraulic behavior of water and polymer, and their mutual interactions within a single computational framework. The governing equations include equilibrium of stresses with damping and continuity equations for water flow and polymer infiltration. Stress-controlled permeability is introduced, which links absolute permeability and water permeability coefficients to the components of the principal stress tensor. Originality of the model lies in several aspects: it captures the time-dependent evolution of the disturbed zone as the polymer hardens, explicitly accounts for the delayed onset of reinforcement, and incorporates stress-controlled permeability reflecting realistic fracture opening and closure under variable stress states. In addition, the model parameters are linked directly to engineering practice, such as the delay before bolt installation and the duration of injection. The problem is solved in an elasto-plastic formulation using finite element discretization.

Computational experiments demonstrate that the injection process produces a strengthened zone of rock with markedly reduced permeability and enhanced stability, effectively transforming weak fractured strata into a low-permeability support reinforced by the rockbolt. The analysis confirms that the model can reproduce polymer hardening, changes in stress distribution, and the progressive reduction of hydraulic conductivity around the bolt. The framework therefore offers a practical tool for designing support systems in underground excavations driven through weak, water-saturated formations, where both structural stability and hydraulic sealing are required. Further refinement of polymer hardening kinetics, incorporation of rock mass anisotropy, and experimental calibration of parameters are suggested as directions for future research.

Keywords: injection rockbolt, rock deformation, polymer injection, groundwater inflow, numerical simulation.

1. Introduction

Injection rockbolts (a specialized type of grouted rockbolt designed to deliver polymer grout into fractured rock) are widely recognized as key support elements for underground excavations, particularly in weak, fractured, or water-bearing formations. They are applied to prevent collapses, stabilize excavation boundaries, reduce deformation, and create hydraulic or gas-sealing barriers in highly permeable zones. The performance of such systems is governed by the mechanical properties of the rock mass, the in situ stress field, and the characteristics of the grout.

In recent years, polymer-based grouts have attracted growing attention due to their superior fluidity, faster strength development, reliable performance under saturated conditions, and stronger adhesion to rock compared with conventional cementitious materials. Their ability to penetrate finer fractures and crushed zones enables more uniform reinforcement and improved sealing efficiency [1–3].

Designing effective injection rockbolts in weak, water-bearing ground requires consideration of three strongly coupled processes: rock mass deformation, groundwater flow, and grout migration during injection. These interactions are highly interdependent – deformation modifies rock permeability, fluid flow influences the stress–strain state, grout penetration depends on hydraulic properties, and hardening alters the mechanical response of the grouted zone. A realistic assessment of rockbolt performance therefore requires an integrated multiphysical model.

Received: 10.07.2025 Accepted: 15.09.2025 Available online: 19.09.2025

The finite element method (FEM) provides a robust and versatile framework for such analyses, as it can capture geometric complexity, nonlinear material behaviour, transient hydro-mechanical interactions, and heterogeneous rock properties [4, 5]. FEM has been successfully applied to rock deformation [6, 7], groundwater flow in fractured media [8], coupled fluid–rock interactions around excavations and tunnels [9–12], cement grouting [13], and polymer injection in deforming rock masses [14–16]. However, a comprehensive FEM study that simultaneously considers rock deformation, groundwater flow, and polymer injection remains limited.

The aim of this study is therefore to develop a coupled mathematical model of rock deformation, groundwater flow, and polymer injection, and to apply FEM to analyze these processes.

To achieve this goal, the following tasks were undertaken:

- to develop a coupled mathematical model of rock deformation, groundwater inflow into a roadway driven in weak water-bearing rocks, and polymer injection during the installation of an injection rockbolt;
- to apply FEM to analyze associated stress distribution, permeability evolution, grout flow and hardening, and the resulting reinforcement and sealing effects around the bolt.

2. Methods

2.1 Fundamental equations and boundary conditions

The interaction between rock mass deformation, groundwater flow, and polymer grout infiltration in fractured zones stabilized with rockbolts is represented through a system of governing equations [15]:

$$c_{\mathrm{g}} \frac{\partial u_i}{\partial t} = \sigma_{ij,j} + X_i(t) + P_i(t);$$

$$\frac{\partial p}{\partial t} = \frac{k_{\mathrm{w}}}{\mu_{\mathrm{w}} \cdot \beta_{\mathrm{w}} \cdot \mathrm{m}} \left(\frac{\partial^2 p}{\partial x^2} + \frac{\partial^2 p}{\partial y^2} \right);$$

$$\frac{\partial p_{\mathrm{p}}}{\partial t} = \frac{k}{\mu_{\mathrm{p}} \cdot \beta_{\mathrm{p}} \cdot \mathrm{m}} \left(\frac{\partial^2 p_{\mathrm{p}}}{\partial x^2} + \frac{\partial^2 p_{\mathrm{p}}}{\partial y^2} \right) + \mathrm{q}(t),$$

where c_{g} – the damping coefficient, kg/(m³·s); t – time, s; u_i – displacement, m; $\sigma_{ij,j}$ – the derivatives of the stress tensor components with respect to x and y, Pa/m; $X_i(t)$ – the projections of external forces acting per unit rock volume, N/m³; $P_i(t)$ – the projections of forces arising from water and polymer pressures in the fracture network, N/m³; p – water pressure, Pa; k – the absolute permeability, m²; k_{w} – water permeability, m²; p_{p} – polymer pressure, Pa; μ_{w} and μ_{p} – the viscosities of water and polymer, respectively, Pa·s; β_{w} and β_{p} – the compressibilities of water and liquid polymer, respectively, Pa^{-1}; m – porosity, %; q(t) – the foaming function.

The analysis is carried out in an elastoplastic framework. The transition of rocks into a fractured state is mathematically described using the Coulomb–Mohr strength criterion.

The initial and boundary conditions are defined as:

$$\sigma_{yy}\big|_{t=0} = \gamma H; \quad \sigma_{xx}\big|_{t=0} = \lambda\gamma H; \quad p_{\mathrm{p}}\big|_{t=0} = 0.1 \text{ MPa}; \quad p\big|_{t=0} = (h + y_0 - y)\rho g;$$
$$u_x\big|_{\Omega_1} = 0; \quad u_y\big|_{\Omega_2} = 0; \quad p_{\mathrm{p}}\big|_{\Omega_3} = p_0; \quad p\big|_{\Omega_4} = 0.1 \text{ MPa},$$

where γ – the average unit weight of the overlying strata, N/m³; H – excavation depth, m; λ – the lateral earth pressure coefficient; h – the piezometric head, m; y_0 – the coordinate of the finite element mesh center, m; ρ – water density, kg/m³; g – gravitational acceleration, m/s²; p_0 – the injection pressure, Pa; Ω_1 – represents vertical external boundaries, Ω_2 – horizontal internal boundaries, Ω_3 – the filtering section of the borehole wall; Ω_4 – the tunnel contour.

For stress-state assessment, two dimensionless geomechanical indicators are employed: $Q^* = (\sigma_1 - \sigma_3)/\gamma H$, denoting the relative principal stress differential, and $P^* = \sigma_3/\gamma H$, reflecting the rock failure potential.

2.2 Injection rockbolt model

In practice, injection rockbolts are commonly installed with a delay of several meters behind the roadway face (typically ~5 m). During this period, the surrounding rock undergoes stress redistribution and partial unloading, which increases fracture permeability. To realistically simulate polymer injection, the numerical model initiates this process not at the excavation moment but with reference to the elapsed time since face advance. The volume expansion of the polymer, caused by mixing and subsequent chemical reactions, is incorporated through a source term q(t) in the fluid flow equation.

As the polymer penetrates and hardens within fractures and voids, the mechanical and hydraulic properties of the treated rock mass evolve. In the model, the compressive strength and elastic modulus of rock elements progressively increase toward the hardened polymer values, while permeability decreases to zero within the filled fracture–pore space ($k \to 0$, $k_{\mathrm{w}} = 0$). Outside this zone, the natural permeability is preserved.

The steel injection tube is assumed to act as a load-bearing rockbolt only after complete grout hardening. Thus, the reinforcing effect of the bar finite elements is activated at $t_{\mathrm{reinf}} = t_{\mathrm{start}} + t_{\mathrm{end}} + t_{\mathrm{hard}}$, where t_{start} – injection start time, s; t_{end} – injection duration, s; t_{hard} – polymer hardening time, s.

2.3 Permeability model

The geometry and extent of the reinforced zone are controlled by the distribution of permeability around the rockbolt. Excavation generates new fractures and modifies the initial permeability k_0, which is further affected by stress redistribution and excavation-induced damage. To capture this, a technological permeability field k_{tech} ex-

pressed as a function of stress tensor components [14] is superimposed on the natural one:

$$k = k_0 + k_{\text{tech}}\left(t,\ Q^*,\ P^*\right).$$

In each finite element node:

$$k_{\text{tech}} = \begin{cases} 0, \text{ if } Q^* < 0.4; P^* > 0.4; \\ A, \text{ if } 0.4 < Q^* < 0.6;\ P^* < 0.4; \\ e^{0.26Q^* - 4.65} + A, \text{ if } 0.6 < Q^* < 1.0;\ P^* < 0.4; \\ k_{\max}, \text{ if } Q^* > 1.0;\ \ P^* < 0.4, \end{cases}$$

where $k_{\max}$ – permeability of completely fractured rock, m^2; $A = k_{\max}\cdot(1\text{-}2{,}5\cdot P^*)$.

Permeability variations are most significant in tectonically disturbed zones, where deformation type largely determines hydraulic properties.

2.4 Finite element model

The finite element mesh consisted of 27,026 nodes and 53,848 three-node triangular elements (Fig. 1), and rockbolts were modelled by the bar finite elements. The model domain (64 m × 64 m) included a roadway (5.2 m × 3.0 m) at its center, with an injection rockbolt positioned at the roof.

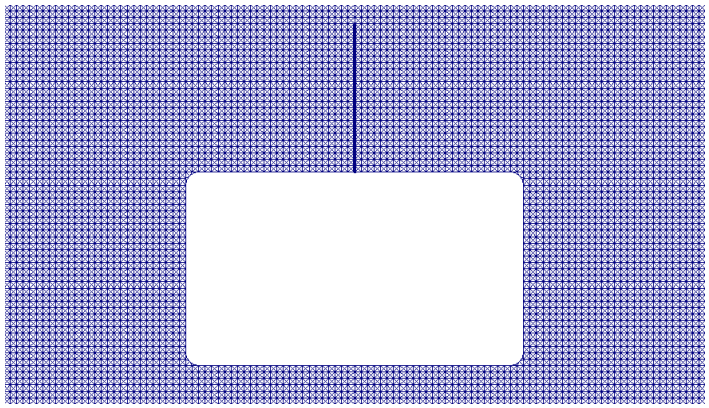

Figure 1 – Finite element model

Plane strain conditions were assumed. Boundary conditions fixed horizontal displacements at the vertical boundaries and vertical displacements at the horizontal boundaries.

2.5 Parameter setting

The reference case considered polymer injection into very weak, excavation-disturbed argillite. Model parameters were: excavation depth H = 800 m; unit weight γ = 25,000 N/m^3; lateral pressure coefficient λ = 1; bolt length = 2.4 m; sealed borehole length = 0.7 m; injection pressure p_0 = 9 MPa; injection start t_{start} = 24 h; injection duration t_{end} = 40 min; hardening time t_{hard} = 40 min; fractured rock permeability $k_{\max}$ = 0.3 mD; intact permeability k_0 = 0.

Properties of the material used are given in Table 1.

Table 1 – Rock and polymer properties

Material	Compressive strength, σ_{cr}, MPa	Elastic modulus, E, MPa	Cohesion, C, MPa
Argillite	10	8000	2,8
Hardened polymer	30	17000	10,0

3. Results and discussion

Figure 2 illustrates the evolution of the stress parameter Q^* together with the zones of inelastic deformation, as well as the distributions of absolute permeability k and water permeability k_w prior to injection and throughout the injection and hardening stages of the polymer.

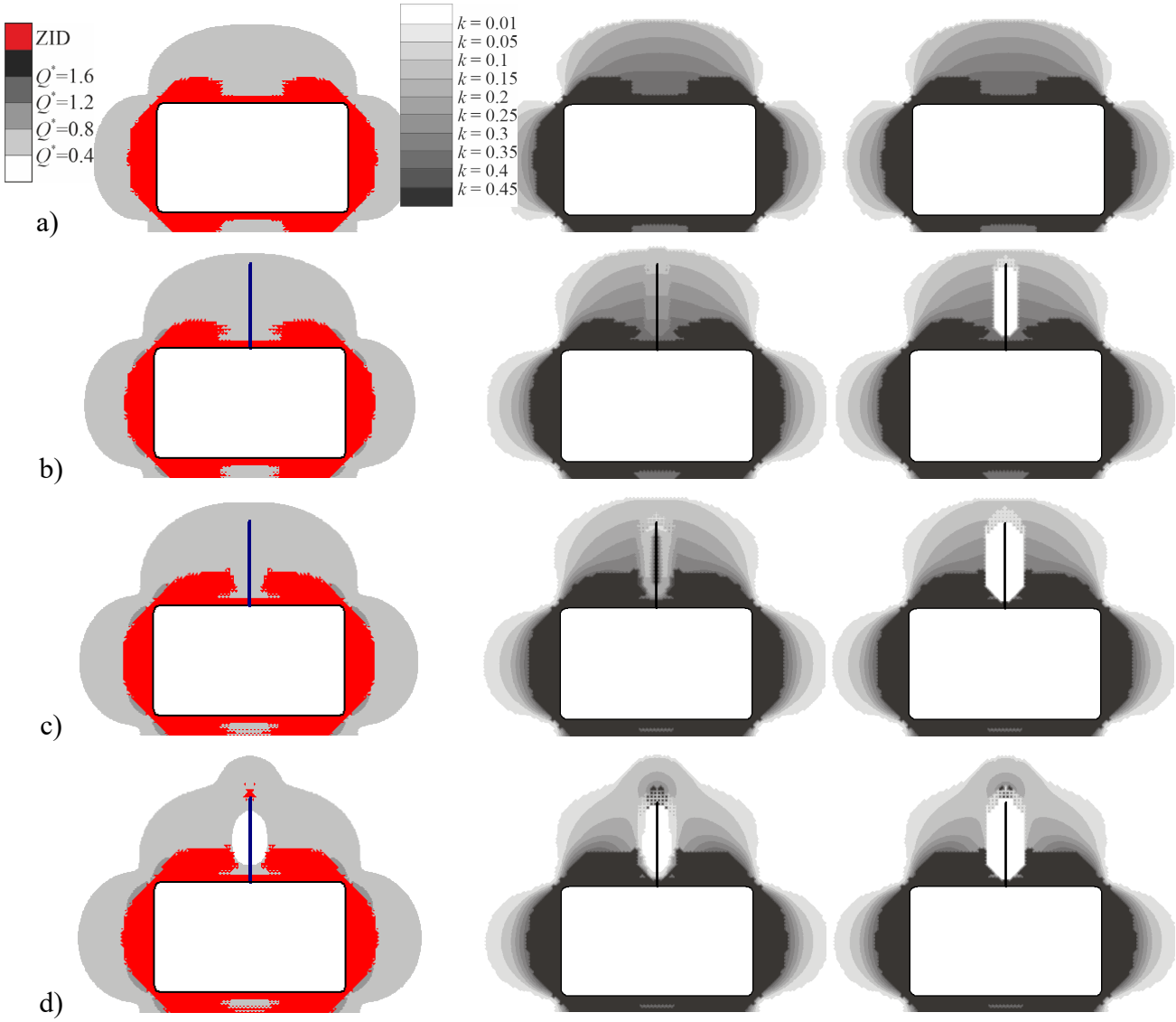

a) prior to injection; b) $\tau = 20$ min; c) $\tau = 60$ min; d) $\tau = 100$ min.

Figure 2 – Evolution of the parameter Q^* with the zones of inelastic deformation (left), distributions of absolute permeability k (center) and water permeability k_w (right)

In the analysis, time τ is defined relative to the onset of injection.

Excavation substantially modifies the stress field within the rock mass. Before the installation of the injection rockbolt, the parameter Q^* increases around the excavation, and the opening becomes encircled by a zone of inelastic deformation (Fig. 2a, left). Consequently, a permeable zone with a depth of up to 2.35 m is formed in the roof at the intended rockbolt location (Fig. 2a, center). Once injection begins, the fracture–pore network progressively fills with polymer, resulting in a reduction of water permeability around the rockbolt (Fig. 2b, right). At τ = 40 min, injection ceases, and polymer hardening initiates, thereby strengthening the weakened rock mass.

At τ = 60 min, the expansion of the inelastic zone adjacent to the rockbolt is stopped. Absolute permeability continues to decrease, while water permeability reduces to zero within the polymer-filled region (Fig. 2c). By τ = 80 min, the polymer has fully solidified, converting the initially weak and unloaded rock into a dense, impermeable composite. From this stage onward, the metallic injection tube functions structurally as a rockbolt. Notably, a distinct reinforced domain emerges around the bolt where $Q^* < 0.4$ (Fig. 2d, left).

The corresponding water pressure field and flow vectors are shown in Figure 3.

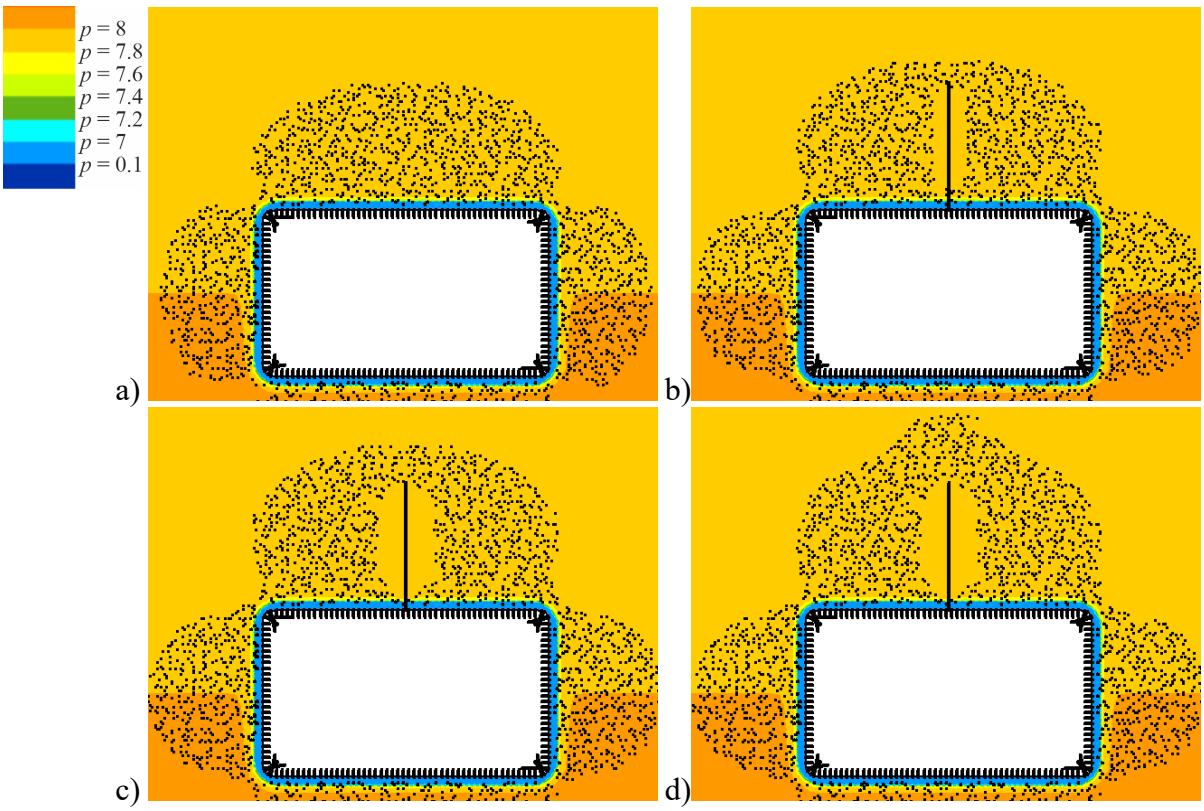

a) prior to injection; b) τ = 20 min; c) τ = 60 min; d) τ = 100 min.

Figure 3 – Water pressure field and flow vectors

Short black dashes indicate filtration pathways, with length proportional to flow velocity. The water movement is confined within the permeable domain: relatively subdued at greater distances but intensifying near excavation boundaries. Once injec-

tion commences (Fig. 3b), an impermeable zone is established adjacent to the bolt, precluding any groundwater movement. With ongoing injection and polymer hardening (Figs. 3b–3d), the extent of this impermeable region progressively expands.

Figure 4 depicts the distribution of normalized polymer pressure p_p/p_0 and the extent of polymer spread. During injection, the reinforced zone expands to a diameter of approximately 1 m, corresponding to an area of ~2.275 m² for the specified initial conditions. The extent of the polymer-filled zone at τ = 20 min and τ = 60 min coincides with the impermeable domains evident in Figures 2 and 3.

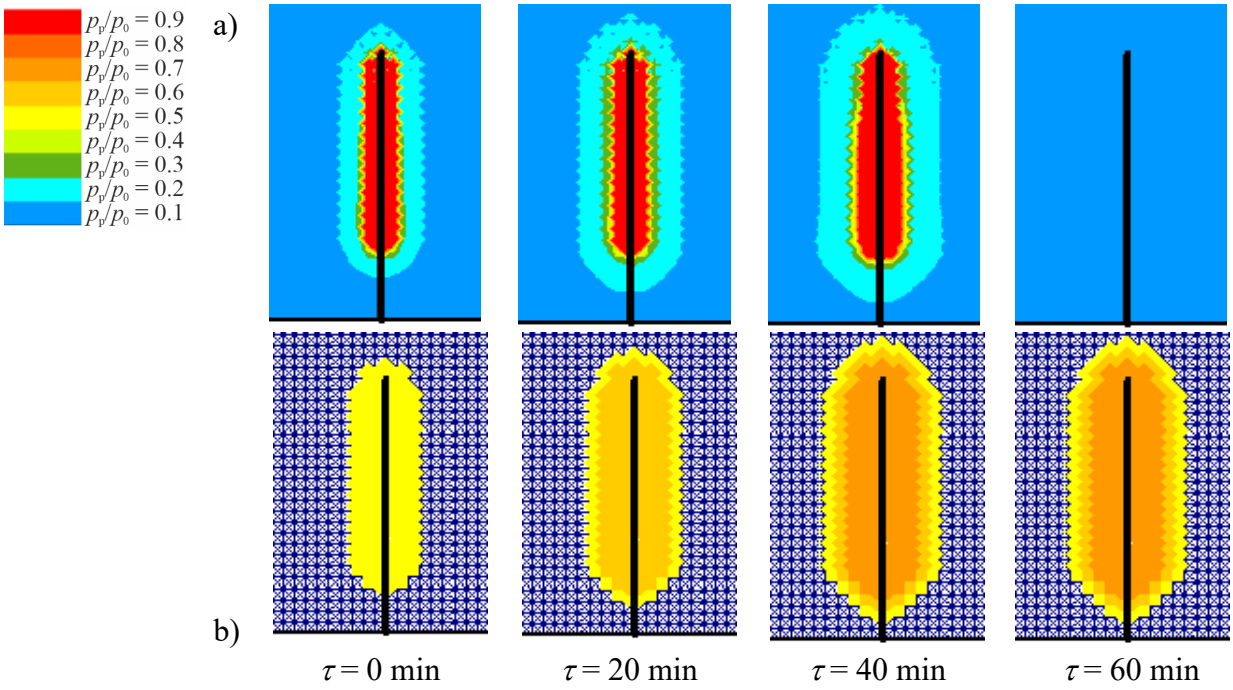

a) normalized polymer pressure p_p/p_0; b) extent of polymer spread.

Figure 4 – Distributions of liquid polymer filtration parameters

In summary, the computational simulation demonstrates that the installation of injection rockbolts leads to the creation of a reinforced support system with markedly reduced relative principal stress differential, enhanced strength, and complete impermeability to groundwater flow.

4. Conclusions

This work introduces a novel model for simulating the coupled processes of rock deformation, groundwater inflow in weak water-bearing strata, and liquid polymer injection associated with the installation of injection rockbolts. The key strengths of the model include:

- integrated framework – capturing mechanical, hydraulic, and chemo-mechanical interactions within a single formulation;
- time-dependent behavior – reflecting property evolution of the fractured zone during polymer hardening and the delayed onset of reinforcement;

- stress-controlled permeability – accounting for realistic fracture opening and closure under varying stress conditions;
- process relevance – parameters linked directly to operational practice (e.g., bolt installation delay, injection duration).

Future developments may focus on refining polymer hardening kinetics, incorporating anisotropy of fractured rock masses, and calibrating parameters through dedicated experiments.

A finite element case study demonstrated the model's capacity to predict stress redistribution, permeability changes, water and polymer flow, and the strengthening of weak rock during bolt installation. The model provides a practical tool for designing reinforcement systems in underground structures driven through weak, water-saturated strata, ensuring both stability and hydraulic impermeability.

Conflict of interest

Authors state no conflict of interest.

REFERENCES

1. MINOVA (2025), "Injection Chemicals. CarboPur WF two-component polyurethane injection resin. Technical data sheet.", available at: https://www.minovaglobal.com/emea/products/injection-chemicals, (Accessed 01 August 2025)

2. Li, S., Liu, R., Zhang, Q. and Zhang, X. (2016), "Protection against water or mud inrush in tunnels by grouting: A review", *Journal of Rock Mechanics and Geotechnical Engineering*, no. 8, 753-766. https://doi.org/10.1016/j.jrmge.2016.05.002

3. Wibisono, D.Y., Setiawan, E., Anugrah, C. and Nasution, R. (2018), "Ground consolidation with material injection Case study for collapse rehabilitation in Tambang Emas Cibaliung, Cibitung Decline X/C-5", *10th Asian Rock Mechanics Symposium,* Singapore, 29 October – 3 November 2018, ISRM-ARMS10-2018-032. available at: https://onepetro.org/ISRMARMS/proceedings-abstract/ARMS1018/ARMS1018/ISRM-ARMS10-2018-032/42976 (Accessed 01 August 2025)

4. Zienkiewicz, O.C., Taylor, R.L. and Zhu, J.Z. (2013), *The Finite Element Method: Its Basis and Fundamentals*, Butterworth-Heinemann, Amsterdam, Netherlands.

5. Rust, W. (2012), *Non-Linear Finite Element Analysis in Structural Mechanics*, Springer, Hannover, Germany.

6. Neuner, M., Schreter, M., Gamnitzer, P. and Hofstetter, G. (2020), "On discrepancies between time-dependent nonlinear 3D and 2D finite element simulations of deep tunnel advance: A numerical study on the Brenner Base Tunnel", *Computers and Geotechnics*, no. 119, 103355. https://doi.org/10.1016/j.compgeo.2019.103355

7. Krukovskyi, O.P. (2020), "Formation of elements of the bolting structure for mine workings", *Geo-Technical Mechanics*, no. 151, pp. 27-62. https://doi.org/10.15407/geotm2020.151.027

8. Preisig, G., Dematteis, A., Torri, R., Monin, N., Milnes, E. and Perrochet, P. (2014), "Modelling discharge rates and ground settlement induced by tunnel excavation", *Rock Mechanics and Rock Engineering*, no. 47, pp. 869–884. http://doi.org/10.1007/s00603-012-0357-4

9. Zhang, C., Zhao, Q. and Yu, Y. (2011), "Model of coupled gas flow and deformation process in heterogeneous coal seams and its application", *Journal of Coal Science & Engineering*, no.17(1), pp. 76–80. http://doi.org/10.1007/s12404-011-0114-4

10. Vynohradov, Y.O. (2019), "Investigation of the support effect on the water inflow to the mine working in difficult hydrogeological conditions at the crossing of tectonic displacement", *Physical and technical problems of mining production*, no. 21, pp. 55-66. https://doi.org/10.37101/ftpgp21.01.005

11. Krukovska, V.V. and Vynohradov, Y.O. (2019), "Water stability influence of host rocks on the process of water filtration into mine working with frame and roof-bolting support", *Geo-Technical Mechanics*, no. 147, pp. 54–61. https://doi.org/10.1051/e3sconf/201910900041

12. Krukovskyi, O., Minieiev, S., Krukovska, V. and Yanzhula O. (2024), "Analysis of the influence of initial coal seam permeability on the hydraulic extrusion process", *Geo-Technical Mechanics*, no. 170. pp. 133-143 https://doi.org/10.15407/geotm2024.170.133

13. Xiao, T., Ren, Y., Li, H., Shen, W., Jia, H., Yue, S. and Liu, F. (2025), "Study on the hierarchical grouting reinforcement control of low permeability surrounding rocks of deep roadway", *Energy Science & Engineering*, pp. 1–12. https://doi.org/10.1002/ese3.70199

14. Krukovska, V.V. and Krukovskyi, O.P. (2019), "Numerical simulation of coupled processes at injection of strengthening compositions in cracked rock with injection anchors", *Geo-Technical Mechanics*, no. 149, pp. 100-110. https://doi.org/10.15407/geotm2019.149.100

15. Krukovskyi, O.P., Krukovska, V.V. and Vynohradov, Y.O. (2023), "The use of injection rock bolts in the mining and geological conditions of Ukrainian coal mines", *Key trends of integrated innovation-driven scientific and technological development of mining regions*, Universitas Publishing, Petroșani, Romania, pp. 387-422. available at: http://ep3.nuwm.edu.ua/id/eprint/25914 (Accessed 01 August 2025)

16. Slashchov, I., Slashchova, O., Seleznov, A., Shmyglov, V., Kryvenko, Ye. and Brizheniuk, V. (2024), “Justification of the parameters of injection rock hardening zones around mining workings and buried structures of critical infrastructure”, *Geo-Technical Mechanics*, no. 170, pp. 165-180. https://doi.org/10.15407/geotm2024.170.165

About the author

Krukovska Viktoriia, Doctor of Technical Sciences (D. Sc), Senior Researcher, Senior Researcher in Department of Dynamic Manifestations of Rock Pressure, M.S. Poliakov Institute of Geotechnical Mechanics of the National Academy of Sciences of Ukraine (IGTM of the NAS of Ukraine), Dnipro, Ukraine, vikakrukk@gmail.com ***(Corresponding author)***, ORCID ***0000-0002-7817-4022***

СКІНЧЕННО-ЕЛЕМЕНТНИЙ АНАЛІЗ ДЕФОРМУВАННЯ, ФІЛЬТРАЦІЇ ҐРУНТОВИХ ВОД ТА НАГНІТАННЯ ПОЛІМЕРІВ ЗА ДОПОМОГОЮ ІН’ЄКЦІЙНИХ АНКЕРІВ

Круковська В.В.

Анотація Це дослідження представляє нову модель скінченних елементів для моделювання зв'язаних процесів деформації гірських порід, притоку ґрунтових вод та ін'єкції полімеру під час встановлення ін'єкційних анкерів у слабкі водоносні пласти. Модель інтегрує механічну реакцію гірського масиву, гідравлічну поведінку води та полімеру, а також їх взаємну взаємодію в рамках єдиної обчислювальної бази. Визначальні рівняння включають рівновагу напружень із затуханням, а також рівняння нерозривності для фільтрації води та полімеру. Введено проникність, контрольовану напруженнями, яка пов'язує абсолютні коефіцієнти проникності та коефіцієнти водопроникності з компонентами тензору головних напружень. Оригінальність моделі полягає в кількох аспектах: вона фіксує залежну від часу еволюцію порушеної зони, коли полімер твердне, явно враховує затримку початку армування та включає проникність, контрольовану напруженнями, що відображає реалістичне відкриття та закриття тріщин за змінних напружених станів. Крім того, її параметри безпосередньо пов'язані з інженерною практикою, такими як затримка перед встановленням анкера та тривалість ін'єкції. Задача вирішується в пружно-пластичній постановці з використанням дискретизації скінченних елементів.

Обчислювальні експерименти показують, що процес ін'єкції створює зміцнену зону гірських порід зі значно зниженою проникністю та підвищеною стійкістю, ефективно перетворюючи слабкі тріщинуваті пласти на опору з низькою проникністю, армовану анкером. Аналіз підтверджує, що модель може відтворювати затвердіння полімеру, зміни розподілу напружень та поступове зниження гідравлічної провідності навколо анкера. Таким чином, ця структура пропонує практичний інструмент для проектування систем кріплення в підземних виробках, що прокладаються через слабкі, водонасичені формації, де потрібна як структурна стабільність, так і гідравлічна герметизація. Подальше вдосконалення кінетики затвердіння полімерів, врахування анізотропії гірської маси та експериментальне калібрування параметрів пропонуються як напрямки для майбутніх досліджень.

Ключові слова: ін’єкційний анкер, деформування порід, нагнітання полімеру, фільтрація ґрунтових вод, чисельне моделювання.